



Giagkoulovits, C., Al-Rawhani, M. A., Cheah, B. C., Martin, C., Busche, C., Cronin, L. and Cumming, D. R.S. (2017) Hybrid Amperometric and Potentiometric Sensing Based on a CMOS ISFET Array. In: IEEE Sensors 2017, Glasgow, UK, 30 Oct - 01 Nov 2017, ISBN 9781509010127.

There may be differences between this version and the published version. You are advised to consult the publisher's version if you wish to cite from it.

<http://eprints.gla.ac.uk/146644/>

Deposited on: 29 August 2017

Enlighten – Research publications by members of the University of Glasgow_
<http://eprints.gla.ac.uk>

Hybrid Amperometric and Potentiometric Sensing Based on a CMOS ISFET Array

Christos Giagkoulovits, Mohammed A. Al-Rawhani, Boon C. Cheah, Christopher Martin, Christoph Busche, Leroy Cronin and David R.S. Cumming
College of Science and Engineering
University of Glasgow
Glasgow, United Kingdom
c.giagkoulovits.1@research.gla.ac.uk

Abstract—Potentiometry and amperometry are some of the most important techniques for electroanalytical applications. Integrating these two techniques on a single chip using CMOS technology paves the way for more analysis and measurement of chemical solutions. In this paper, we describe the integration of electrode transducers (amperometry) on an ion imager based on an ISFET array (potentiometry). In particular, this integration enables the spatial representation of the potential distribution of active electrodes in a chemical solution under investigation.

Keywords—potentiometry; amperometry; microelectrode; CMOS; ISFET

I. INTRODUCTION

Electrochemical sensing is broadly used in chemical and biological research. Three modes of electrochemical analysis are most commonly used, namely potentiometry, amperometry and impedance spectroscopy [1]. Popular applications of the technology include point-of-care tests, gas sensing, DNA sequencing, food quality tests, electrophysiological measurements and scanning probe microscopy techniques [2]. Most applications rely only on one analysis mode, however in order to study more complex systems the combination of two modes is sometimes required. An example is the combination of potentiometry and amperometry for the study of electrode kinetics on an active amperometric electrode (scanning electrochemical potential microscopy (SECPM)) [3].

Conventionally large-scale electrodes are used to perform electrochemical analysis. With the advancement on microelectronics, complementary metal oxide semiconductor (CMOS) technology has enabled implementing miniaturized integrated CMOS versions of electrochemical transducers. For example, potentiometry has been used on CMOS by miniaturizing the glass electrode to the ion-sensitive field effect transistor (ISFET). This has led to the creation of an ion imaging camera [4]. On the other hand, when amperometry was the targeted mode on CMOS technology, ultramicroelectrodes and reading circuits were integrated in array formats. The monolithic devices exhibited improved accuracy and steady-state diffusion currents [5], [6].

An ISFET operates in a liquid environment, using a reference electrode held at a constant potential and a MOSFET transistor that has its gate interface floating. The ionic composition of the sample influences the signal at the gate,

thus it controls the behaviour of the transistor, operating as a potentiometric indicator electrode. On the other side, microelectrodes can be used in conjunction with a potentiostat, as an amperometric device. A known potential difference is applied between them causing redox processes that produce a readout current proportional to the analyte concentration [2].

In this paper we present a study of integrating two modes, namely potentiometry and amperometry on CMOS technology. Local charge distribution on and around integrated ultramicroelectrodes was recorded by our ion imager. This feature enabled us to monitor the behaviour of the electrical double layer (EDL) along the course of a cyclic voltammogram.

The rest of this paper is organized as follows. In section II, the ISFET as a potentiometer is described together with its response at different pH concentrations. This is followed in section III by a description of the electrode transducers and their characteristics. The response of the combined potentiometric and amperometric system is then described and explained in section IV. In section V the paper is concluded.

II. ISFET

The ISFET sensor is designed using a source follower

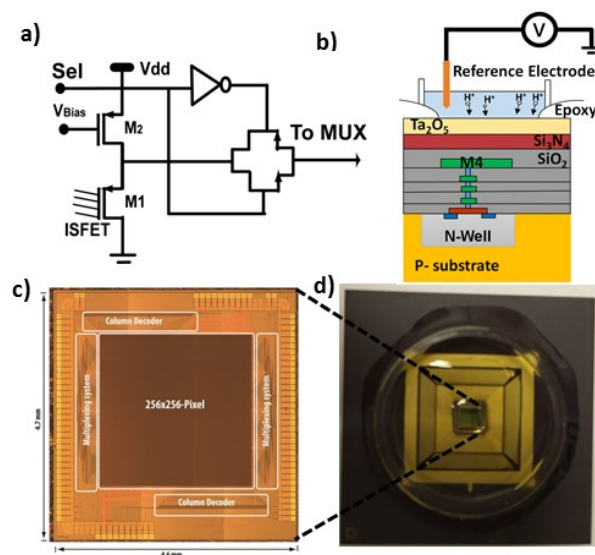


Fig. 1 The ISFET sensor array (a) pixel electronic circuit, (b) cross-sectional operation, (c) optical micrograph and (d) encapsulation of the chip [4].

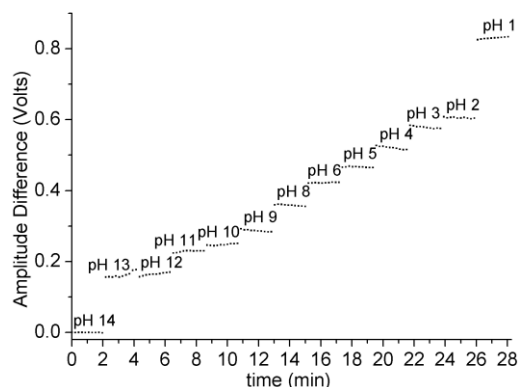


Fig. 2 Serial pH measurements representation.

transistor configuration (M_1 & M_2), where, M_1 has a floating gate connected to a four metal layer stack in contact with the top passivation layer in the CMOS process (SiO_2 and Si_3N_4) as illustrated in Fig. 1(a) and 1(b). In solution, this layer acts as a dielectric membrane (an insulator) in which a change in the concentration of ions changes the gate voltage of M_1 and therefore varies the output accordingly. In an array configuration, each sensor “pixel” incorporates a transmission gate to select the ISFET for readout. The chip integrates a 256×265 ISFET array that employs two 7-bit decoders and two 3-bit analogue multiplexers to scan through the entire array. The chip was fabricated using a 350 nm CMOS process provided by ams AG [4]. Its total area measures $4.5\text{mm} \times 4.5\text{mm}$ of which the active area is $3.8\text{mm} \times 3.8\text{mm}$ and the ISFET “pixel” size is $10.2\ \mu\text{m} \times 10.2\ \mu\text{m}$ (Fig. 1(c)). In order to make the chip more sensitive to a wide range of ions, it was post-processed with a thin layer of Ta_2O_5 layer deposited on top of the chip’s active area, as shown in Fig. 1(b). For testing its performance, the chip was bonded and packaged using epoxy for its contacts to be insulated and withstand wet experiments (Fig. 1(c)). Fig. 2 shows the response of the chip to a range of different pH concentrations ranging from pH2-pH14, measured with an NI© based acquisition system. An average sensitivity of 45 mV/pH was recorded.

III. ELECTRODE TRANSDUCERS

Microelectrodes can be arranged in a three electrode system, namely counter electrode (CE), reference electrode (RE) and working electrode (WE). A potential difference is applied between the CE and the WE, while the RE helps maintain a controlled potential at the vicinity of the WE according to $V_{\text{controlled}} = V_{\text{WE}} - V_{\text{RE}}$ [7].

A microelectrode arrangement of three parallel lines of a $10\ \mu\text{m}$ width and long enough to cover a large number of ISFETs was deposited on a dummy sample. The sample was prepared with an insulating Si_3N_4 surface, prepared by an inductively coupled plasma chemical vapour deposition. The microelectrodes were patterned by thermal evaporation of $20\ \text{nm}$ Ti and $400\ \text{nm}$ Au bilayer followed by an LOR/positive photoresist (S1818) liftoff process and are depicted in Fig. 3(a). The sample was wire bonded and a fluid container was formed to enable electroanalytical measurements.

In order to perform potential scanning electrochemical measurements, called cyclic voltammograms (CVs), a solution consisting of an acetonitrile solvent, 0.1M TBAPF6 and 10mM

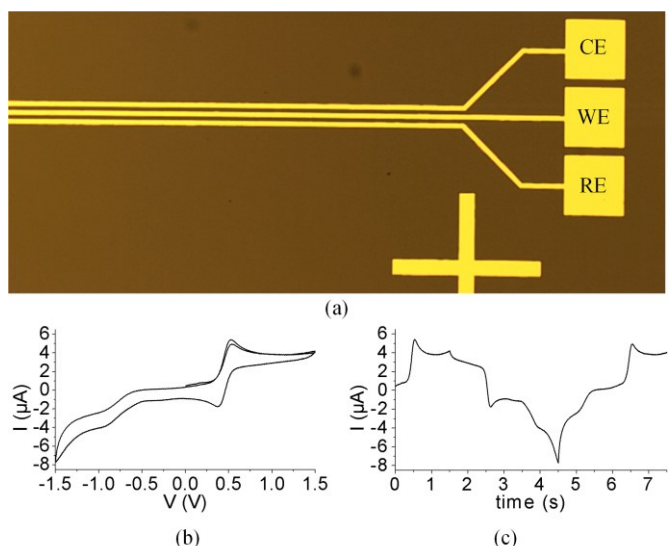


Fig. 3 (a) Optical micrograph of the electrodes deposited on a dummy Si_3N_4 . (b) Cyclic voltammogram of 10mM ferrocene in acetonitrile with 0.1M TBAPF6 and (c) the same measurement resolved in time.

ferrocene was placed in the test container. Cyclic voltammetry is an amperometric potential scanning technique which employs a triangular waveform at $V_{\text{controlled}}$. An external commercial CHI600D potentiostat from CH Instruments was used to perform measurements at a $1\ \text{V/s}$ scan rate. The results were plotted in a CV against voltage, as shown in Fig. 3(b). The peaks around $400\ \text{mV}$ are characteristic of ferrocene’s half-wave potential [8]. Even though the chosen scan rate has a high value the response demonstrates a typical CV, due to the use of microelectrodes. The CV was unravelled and plotted against time in Fig. 3(c).

IV. INTEGRATION

In order to integrate the two sensing technologies on a single chip, the same microelectrode arrangement was photolithographically patterned and the metal bilayer was deposited on the active area of the ISFET array chip, as shown in Fig. 4. Each integrated electrode covers a column of ISFETs on the chip. In this configuration, electrodes form two regions on the surface of the chip. One region operates as normal with ions affecting the insulator interface potential and changing the ISFETs’ gate voltage. The other region includes ISFETs exactly underneath the electrodes that form two parallel plates of a capacitor. The voltage supplied by the potentiostat drives this capacitor and consequently the ISFET output.

The integrated chip was operated and tested in the ferrocene rich solution previously described, using the setup depicted in Fig. 5(a). In this arrangement, the ISFET chip was operated as described in Section II, whereas the electrodes

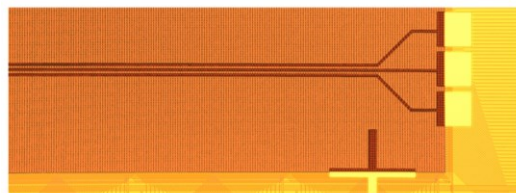


Fig. 4 Optical micrograph of the electrodes deposited on top of the CMOS ISFET array.

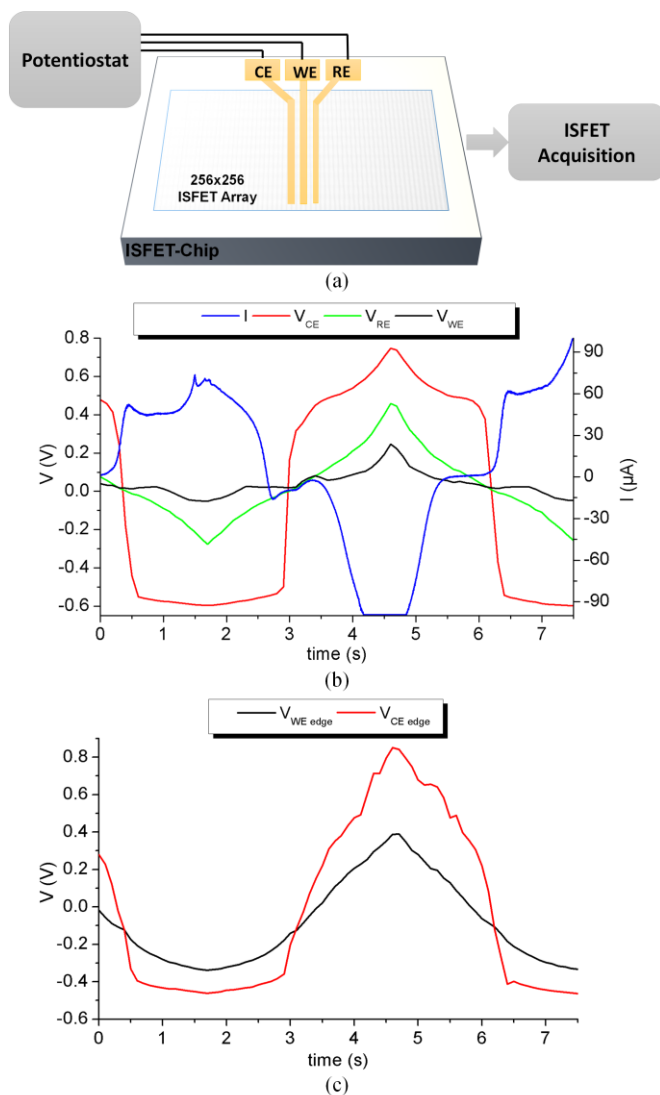


Fig. 5 (a) Conceptual description of the combined measurement system. Combined amperometric and potentiometric measurement of a cyclic voltammogram (b) at the electrodes and (c) over the diffusion areas.

were connected to the commercial potentiostat used in Section III. As shown in Fig. 5(b), it can be observed that the current measured at the WE by the potentiostat exhibited the same behaviour as the dummy sample measurement shown in Fig. 3(c). This means that at this high scan rate, microelectrode properties made possible the reduction of background current and a Faradaic response was maintained over the course of the measurement.

To monitor the electrical double layer formation, individual ISFET measurements were taken from different regions of the active area and then averaged per region. In Fig. 5(b) signals taken from ISFETs at the electrode areas are plotted against time and are inverted in relation to the measured current as the latter is measured with a direction from the WE to the solution. As expected, potential values at the CE exhibited a higher magnitude than the other two, accounting for the potential (iR) drop due to the electrolyte resistance. The measured potential at the RE is a transformed version of the waveform function set

by the potentiostat. The signal is converted by to the oxide capacitance between the electrode and the transistor gate of the ISFET and can be corrected if multiplied by a factor. When measured at the WE the potential values exhibit a correlation to the CE values, indicating a possible diffusion overlap.

The potentials of areas at the edges of the electrodes, where the ISFET array monitors the ionic activity were plotted separately in Fig. 5(c). The potential drops at the edge of the CE due to EDL impedances. The area between the WE and the RE at the WE edge demonstrates a response that lies between $V_{CE\ edge}$ and V_{RE} with its values affected by the ionic diffusion.

V. CONCLUSION

In this paper we presented the integration of two electrochemical sensing technologies on CMOS, namely, potentiometry and amperometry. We used electrode transducers to induce CVs in a liquid solution and an ISFET sensor array to observe the potential distribution on chip. The obtained results confirmed that the ISFET was able to observe a potential gradient across the chip, which is characteristic of the three electrode system. This study was conducted using simple metal structures deposited on an active sensor surface, future work is to scale up the number of electrodes to an array format as well as integrate their potentiostat in the same chip with the ISFETs. The two-sensor array would enable interactive measurements with local control and higher sensitivity. This can lead to the development a non-invasive on-chip implementation of SECPM [3].

VI. ACKNOWLEDGEMENTS

All our datasets can be accessed here: <http://dx.doi.org/10.5525/gla.researchdata.438>.

REFERENCES

- [1] H. Li, X. Liu, L. Li, X. Mu, R. Genov, and A. Mason, "CMOS electrochemical instrumentation for biosensor microsystems: A review," *Sensors*, vol. 17, no. 1, p. 74, Dec. 2016.
- [2] A. J. Bard, Ed., *Encyclopedia of Electrochemistry*. Weinheim, Germany: Wiley-VCH Verlag GmbH & Co. KGaA, 2007.
- [3] C. Hurth, C. Li, and A. J. Bard, "Direct probing of electrical double layers by scanning electrochemical potential microscopy," *J. Phys. Chem. C*, vol. 111, no. 12, pp. 4620–4627, Mar. 2007.
- [4] B. C. Cheah *et al.*, "An integrated circuit for chip-based analysis of enzyme kinetics and metabolite quantification," *IEEE Trans. Biomed. Circuits Syst.*, vol. 10, no. 3, pp. 721–730, Jun. 2016.
- [5] I. L. Jones, P. Livi, M. K. Lewandowska, M. Fiscella, B. Roscic, and A. Hierlemann, "The potential of microelectrode arrays and microelectronics for biomedical research and diagnostics," *Anal. Bioanal. Chem.*, vol. 399, no. 7, pp. 2313–2329, Mar. 2011.
- [6] J. Rothe, O. Frey, A. Stettler, Y. Chen, and A. Hierlemann, "Fully integrated CMOS microsystem for electrochemical measurements on 32×32 working electrodes at 90 frames per second," *Anal. Chem.*, vol. 86, no. 13, pp. 6425–32, Jul. 2014.
- [7] A. Bard and L. Faulkner, *Electrochemical Methods: Fundamentals and Applications*. John Wiley & Sons, Inc, 2001.
- [8] N. G. Tzierkezos and U. Ritter, "Electrochemical impedance spectroscopy and cyclic voltammetry of ferrocene in acetonitrile/acetone system," *J. Appl. Electrochem.*, vol. 40, no. 2, pp. 409–417, Feb. 2010.